ADVANCED FUNCTIONAL MATERIALS

Supporting Information

Synergetic Hybridization Strategy to Enhance the Dynamicity of Poorly Dynamic CO_2-derived Vitrimers achieved by a Simple Copolymerization Approach

Guillem Seychal, Marta Ximenis, Vincent Lemaur, Bruno Grignard, Roberto Lazzaroni, Christophe Detrembleur, Haritz Sardon*, Nora Aranburu* and Jean-Marie Raquez*

Synergetic Hybridization Strategy to Enhance the Dynamicity of Poorly Dynamic CO$_2$-derived Vitrimers achieved by a Simple Copolymerization Approach

Guillem Seychal[1,2], Marta Ximenis[2], Vincent Lemaur[3], Bruno Grignard[4,5], Roberto Lazzaroni[3], Christophe Detrembleur[4], Haritz Sardon[*2], Nora Aramburu[2], and Jean-Marie Raquez[†1]

[1] *Laboratory of Polymeric and Composite Materials, Center of Innovation and Research in Materials and Polymers (CIRMAP), University of Mons, Place du Parc 23, Mons, 7000, Belgium*
[2] *POLYMAT and Department of Advanced Polymers and Materials: Physics, Chemistry, and Technology, Faculty of Chemistry, University of the Basque Country UPV/EHU, Paseo Manuel de Lardizabal 3, Donostia-San Sebastián, 20018, Spain*
[3] *Laboratory for Chemistry of Novel Materials, Research Institute for Materials Science and Engineering, University of Mons, Place du Parc 23, Mons, 7000, Belgium*
[4] *Department of Chemistry, Center for Education and Research on Macromolecules (CERM), University of Liège, Sart-Tilman, B6A, Liège, 4000, Belgium*
[5] *FRITCO$_2$T Platform, University of Liege, Sart-Tilman B6a, 4000 Liege, Belgium*

Supplementary Informations

Contents

---

[*]haritz.sardon@ehu.eus
[†]jean-marie.raquez@umons.ac.be

List of Figures

I Experimental Section

I.1 Materials

Ethylene Carbonate, n-butylamine, 1-Dimethylamino-2-propanol, 4-Methyl-2-pentanol, tetrabutylammonium iodide (TBAI),diglycidyl ether of bisphenol A (D.E.R.332, Epoxy Equivalent Weight EEW = 175 g/eq), 4,4'-Methylenebis(N,N-diglycidylaniline) (MDGA, EEW = 112 g/eq) and m-xylylene diamine (mXDA, Amine Hydrogen Equivalent Weight (AHEW) = 68 g/eq) were purchased from Sigma-Aldrich. Trimethylol propane triglycidyl ether (TMPTE, DENACOL EX321, EEW = 140 g/eq), resorcinol diglycidyl ether (RDGE, DENACOL EX201, EEW = 117 g/eq), polyethylene glycol (PEGGE, DENACOL EX851, EEW = 151 g/eq) were kindly provided by DENACOL NAGASE Chemtex. Pentaerythritol polyglycidyl ether (PEPGE, IPOX CL16eco, biobased grade, EEW =163 g/eq), butanediol diglycidyl ether (BDGE, IPOX RD3 eco, EEW = 135 g/eq) and polyglycidyl ether of ethoxylated trimethylolpropane (EOTMPTGE, Ipox CL60, EEW = 380 g/eq) were kindly provided by Ipox Chemicals. Carbon Dioxide was provided by Air Liquide. All chemicals were used as received without any further purification. Carbon Fiber quasi-unidirectional tape (CF-UD100, Pyrofil TR50S 15k, 100 g.m^{-2}) was purchased from Mitsubishi.

I.2 Synthetic and manufacturing procedures

I.2.1 Synthesis of trimethylolpropane triglycidyl carbonate and other cyclic carbonates

Trimethylolpropane tricyclic carbonate (TMPTC, Carbonate Equivalent Weight CEW = 175 g/eq) was synthesized at the kilogram scale from its respective epoxide precursor as described in a previous study [1]. Shortly, TMPTE was introduced in a 2 L high-pressure stainless steel reactor with 2.5 mol% (vs TMPTE) of TBAI as the catalyst. The reactor was closed and stabilized at 80 °C and 110 bar for 24 h. The crude was collected, degassed under vacuum, and used without any purification. The complete conversion was confirmed by ^{1}H-NMR. PEPGE, BDGE, RDGE, and EOTMPTGE were respectively carbonated into Pentaerythritol CC (CEW = 180 g/eq), Butanediol CC (CEW = 157 g/eq), Resorcinol CC (CEW = 158 g/eq), and Ethoxylated Trimethylol propane CC (CEW = 430 g/eq) in a similar protocol.
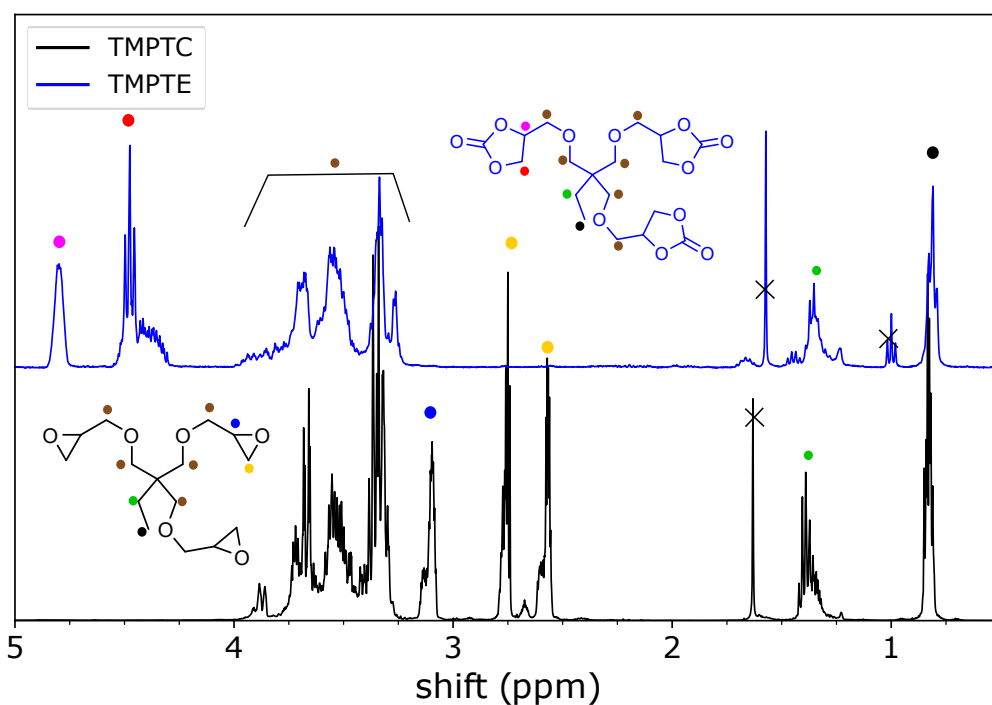
Fig. S 1: ^{1}H-NMR in CDCl$_3$ of the epoxy precursor (TMPTE) and the resulting carbonate (TMPTC)

I.2.2 Synthesis of the 2-hydroxyethyl n-butylcarbamate

In a 25 mL round bottom flask, ethylene carbonate (EC, 1 eq) was mixed with n-butylamine (1.1 eq) and reacted at 60 °C for 24 h under constant stirring. The crude was then dissolved in ethyl acetate and washed with water 3 times to remove the unreacted excess of amine. The product was then dried using anhydrous sodium sulfate. Ethyl acetate was then removed using a rotary evaporator. The obtained product was characterized by ^{1}H-NMR. 2-hydroxyethyl n-butylcarbamate (CDCl$_3$,ppm) : 4.20 (t,CH$_2$), 3.80 (t,CH$_2$), 3.20 (m,CH$_2$), 1.49 (m,CH$_2$) , 1.36 (m,CH$_2$), 0.92 (t,CH$_3$)
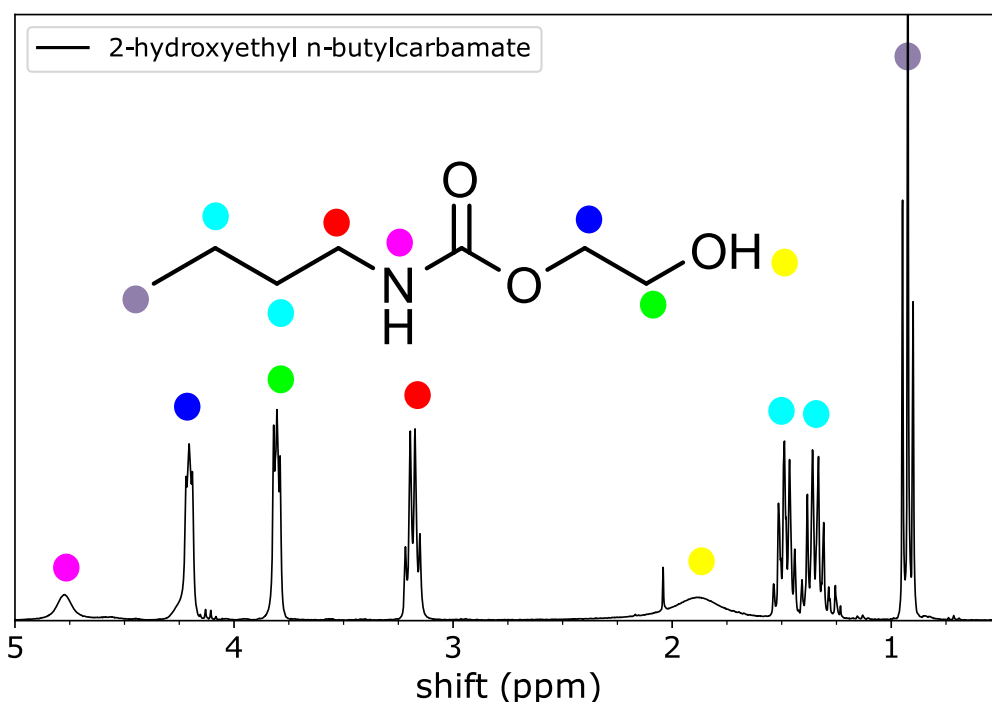
Fig. S 2: ^{1}H-NMR in CDCl$_3$ of the 2-hydroxyethyl n-butylcarbamate model compound

I.2.3 Transcarbamoylation model reaction

Model reactions between the model hydroxyurethane compound (2-hydroxyethyl n-butylcarbamate) and model epoxy compound (1-dimethylamino-2-propanol) were carried out under various temperatures. The two components were mixed in an equimolar ratio and aliquots of the reaction mixture were sampled over time. The reactions were monitored by ^{1}H-NMR in CDCl$_3$ to determine the exchange by following the ethylene glycol signal. Representative NMR spectra for the different model reactions are shown in 3 and 4 together with the resonances used for quantification. For the sake of comparison, the same reaction was conducted with 4-Methyl-2-pentanol which does not possess the catalyzing amine. The reaction was conducted at 120 °C for 24h.

I.2.4 Polymer network formation

The epoxy monomer (resorcinol diglycidyl ether) and the cyclic carbonates (trimethylolpropane triglycidyl carbonate) were mixed and degassed before use. The amine hardener (mXDA) was added in an equimolar ratio between reacting functions. The amount of amine was calculated using eq.1. The mixture was thoroughly hand-mixed for 5 minutes at room temperature and then poured into a PTFE mold. The curing was performed for 2 h at 80 °C followed by a post-curing step of 1 h at 160 °C to guarantee full curing.

$$m_{NH_2} = m_{monomer} \times (\%CC \times \frac{AHEW}{CEW} + \%EP \times \frac{AHEW}{EEW})$$ (1)

I.2.5 Reprocessing of the polymer network

The as-cured thermoset was cut into pieces. The mold was preheated to 180 °C in a press for 30 min. After that, a 6 MPa pressure was slowly applied and maintained for 20 min. The mold was then removed from the press and cooled down at room temperature. The as-obtained film was then removed from the mold and cut for analysis. The samples were also immersed into THF to evidence the welding of the samples via the formation of covalent bonds at high pressure.

I.2.6 Structural composite manufacturing

Unidirectional composite laminates made of 10 plies of carbon fibers were manufactured by hand lay-up and cured by thermocompression. To impregnate the fibers, the polymer mixture was prepared by weighting about 1.2 times the mass of fibers. The plies were stacked in a Teflon-coated steel mold (200x150 mm^2). Between each ply, a layer of resin was applied. The two edges in the mold length were left open to allow air and matrix excess to flow out from the mold. The mold was then placed into a heating press and a pressure of 8 bar was slowly applied to ensure an entire impregnation of the fibers. The plates were then cured under this pressure for 2 h at 80 °C. After unmolding, the post-curing was conducted in an oven at 160 °C for 1 h. Samples were precisely cut from the obtained plates using a metallic guillotine for testing. Before testing, these samples were conditioned at 23 °C and 50% RH to guarantee moisture equilibrium. The fiber mass was estimated from the reinforcement areal weight using eq.(2). Fiber volume fraction (V_f) was calculated using eq.(3) and void content (V_v) was calculated using eq.(4).

$$m_f = n \times A_r \times S \tag{2}$$

$$V_f = \frac{\frac{m_f}{\rho_f}}{\frac{m_f}{\rho_f} + \frac{m_c - m_f}{\rho_m}} \tag{3}$$

$$V_p = 1 - \rho_c \left(\frac{w_m}{\rho_m} + \frac{w_f}{\rho_f} \right) \tag{4}$$

in which n is the number of plies, S is the sample's surface, and A_r is the reinforcement areal weight. ρ_x, m_x, and w_x refer to the density, the mass, and the weight fraction respectively. f subscript refers to fibers, m to the matrix, and c to the composite. Carbon fiber density was fixed at 1.82 g/cm^3 as specified in the supplier technical datasheet. Matrix density values were measured in ethanol using Archimedes's principle.

I.2.7 Reshaping and welding of the cured composites

The reshaping of the composite was conducted in a Teflon-coated V-shaped aluminum mold in a hydraulic press. The mold was first preheated at 180 °C. A unidirectional cured CFRP panel was then put in the mold without pressure for 15 min to preheat. The pressure was slowly applied up to 5 MPa and maintained for 30 min. The press was then water-cooled and the reshaped composites unmolded.

I.2.8 Chemical recovery and recycling of the fibers

The degradation solution was prepared by mixing in a mass ratio of 80:20 glacial acetic acid and hydrogen peroxide (water solution 30 %wt). The composite material (10 g) was roughly cut into large pieces and put in a 250 mL round bottom flask with 250 mL of the oxidative solution. The mixture was heated to 60 °C until complete degradation of the matrix (around 4 h) under constant magnetic

stirring. The fibers were then recovered by filtration and washed several times with deionized water until a neutral pH was obtained. The fibers were then dried overnight in a ventilated oven at 60 °C. The reclaimed fibers were reused as a reinforcement using the hybrid matrix by impregnation under thermo-compression.

I.3   Instrumentation

[1]**H-Nuclear magnetic resonance (NMR)**   measurements were carried out on a Bruker Advance 300 (300 MHz) spectrometer using deuterated chloroform ($CDCl_3$) as solvent at ambient temperature (298 K).

High-resolution mass spectrometry (HRMS)   was measured with a Waters modelo SYNAPTTM G2 HDMSTM, using a Q-TOF detector and negative electrospray ionization ESI+, and elution of the sample was done using $CHCl_3$.

Attenuated total reflection - Fourier-transform infrared spectroscopy (ATR-FTIR)   measurements were performed on a Bruker FTIR Tensor 27 spectrometer. Thirty-two scans per recording were performed over a range of 4000–600 cm^{-1} with a 4 cm^{-1} resolution.

X-ray photoelectron spectroscopy (XPS)   measurements were performed on a Versaprobe III Physical Electronics (ULVAC) system with a monochromatic Al Kα radiation source (1486.7 eV). An initial analysis was carried out to determine the elements present (wide scan: step energy 0.2 eV, pass energy 224 eV) and detailed analyses were carried out on the detected elements (detail scan: step energy 0.05 eV, pass energy 27 eV, time per step 20 ms) with an electron exit angle of 45º. The spectrometer was previously calibrated with Ag (Ag 3d5/2, 368.26 eV). The spectra were fitted using the CasaXPS 2.3.26 software, which models the contributions after a background subtraction (Shirley).

Scanning Electron Microscopy (SEM)   was performed with a HITACHI TM3030Plus Tabletop Scanning Electron Microscope (SEM) at 15 kV. Polymer samples were gold-coated in an SC7620 Mini Sputter Coater (Quorum).

Thermogravimetric Analyses (TGA)   was performed on a TGAQ500 from TA Instruments. About 10 mg of the product was weighed. The analyses were conducted from 25 to 800 °C following a 20 °C/min heating ramp under a N_2 flow of 60 mL.min^{-1}.

Dynamical Mechanical Analyses (DMA)   were conducted on a TA Instruments DMA Q800 in tension mode. Rectangular samples of 20x8x0.8 mm^3 were used. The gauge length was fixed at 10 mm. The DMA analysis was performed from 25 to 180 °C at a 3 °C/min heating rate. 0.1% strain was applied at 1 Hz. The DMA results were used to determine the crosslinking density ($\nu_{E'}$) of samples using rubber elasticity theory as described in eq.(5).

$$\nu_{E'} = \frac{E'_{T_{\alpha+50}}}{3RT_{\alpha+50}} \tag{5}$$

with $T_{\alpha+50}$ being the temperature of the rubbery plateau set 50 K after the α transition taken at the maximum of the tanδ curve, $E'_{T_{\alpha+50}}$ the storage modulus in Pa at the specified temperature and R the perfect gas constant (8.314 J.mol^{-1}K^{-1}).

Stress Relaxation tests were conducted on the DMA Q800 in tension mode. Rectangular samples of 20x8x0.8 mm^3 were used. The gauge length was fixed at 10 mm. Once the specified temperature was reached, the sample was held for 1 min before applying a 1% strain. The strain was kept constant for 60 min or when stress relaxation was reached. Stress relaxation of the dynamic crosslinked network is defined using a Maxwell model as described in eq.(6). The dynamic covalent behavior was highlighted using the Arrhenius relationship by plotting τ^* as a function of 1/T as shown in eq.(7).

$$\frac{G(t)}{G_0} = e^{\frac{-t}{\tau^*}} \tag{6}$$

$$\tau^* = \tau_0 e^{\frac{E_a}{RT}} \tag{7}$$

$$\tag{8}$$

with G being the relaxation modulus in MPa, τ the time constant in second, E_a the activation energy in kJ/mol, R the perfect gas constant (8.314 J.mol^{-1}.K^{-1}), T the temperature in Kelvin.

Tensile Creep was measured in the DMA instrument with the same sample geometry as DMA and stress relaxation. The samples were heated at the desired temperature and maintained for 5 min to ensure equilibrium. Then, a 0.5 MPa stress was applied for 60 minutes, and the strain was recorded.

Monotonic Tensile Test were performed using an INSTRON 5569 testing equipment. Pure polymer materials were tested following the ASTM D638 standard (type V dog-bone shape) with a 2.5 kN cell force. Tests were performed at a 1 mm/min displacement rate up to failure. Young's modulus was calculated by linear regression between 0.1% and 1.0% strain. Composite materials were tested following the ASTM D3039 standard with a 50 kN cell at a 1 mm/min displacement rate up to failure. Samples of dimension 200 x 15 x 0.9 mm^3 were used. The strain was measured using a 50 mm extensometer.

Gel Content (GC) were measureed in triplicates. Three samples of about 20 mg were weighted (m_0) and soaked in a polar tetrahydrofuran (THF). Samples were then collected, and the excess solvent was removed using absorbent paper and then weighted (m_1). The swelling index (SI) was calculated using eq.(9). The same samples were then dried at 80°C under vacuum for 24 h and weighted (m_2). The GC was calculated using eq.(10)

$$SI = \frac{m_1 - m_0}{m_0} * 100 \tag{9}$$

$$GC = \frac{m_2}{m_0} * 100 \tag{10}$$

I.4 Simulation

The free energies of the transcarbamoylation reactions have been estimated at the Density Functional Theory (DFT) level using the B3LYP functional, a 6-31G** basis set and the GD3BJ Grimme's dispersion correction [2] as the energy difference between the sum of the free energies of the DFT-optimized isolated products and that of the reactants. The reported atomic charges have been obtained by fitting the electrostatic potential (ESP charges [3]) calculated at the same level of theory as for the reaction free energies calculations.

II Additional results

II.1 Exchange model reactions

II.1.1 Exchange reaction uncatalyzed
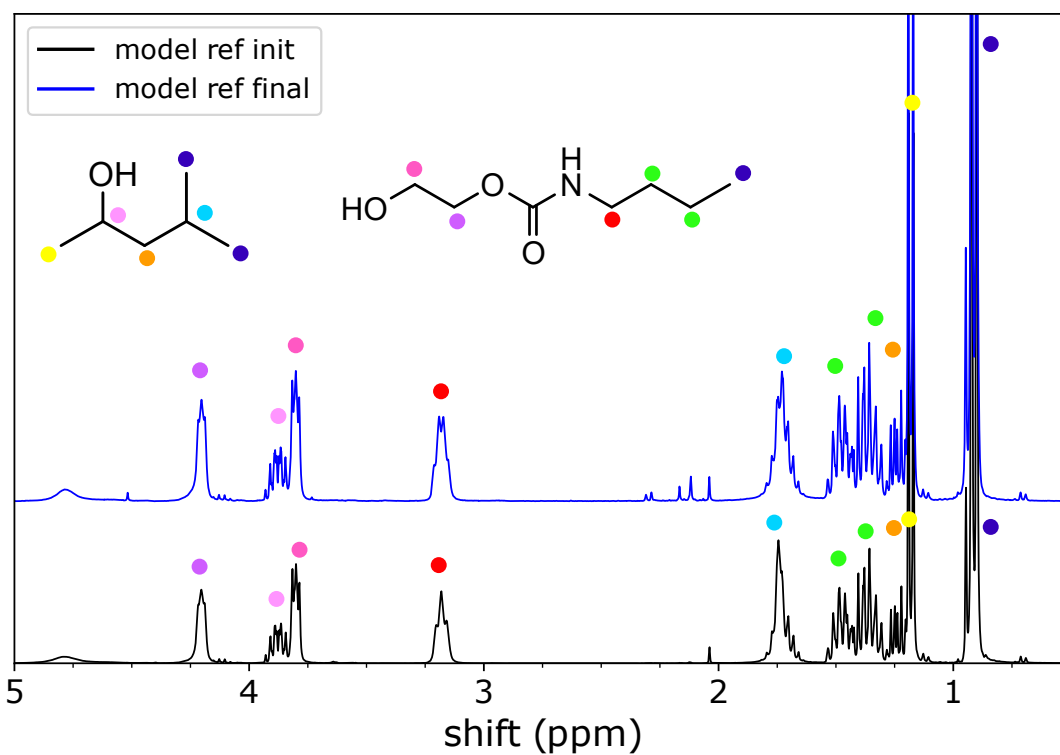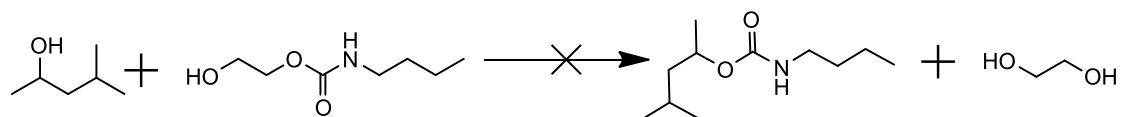
Fig. S 3: ^{1}H-NMR in CDCl$_3$ of the 2-hydroxyethyl n-butylcarbamate model compound with 4-Methyl-2-pentanol before and after 24 h at 120 °C

II.1.2 Exchange reaction self-catalyzed
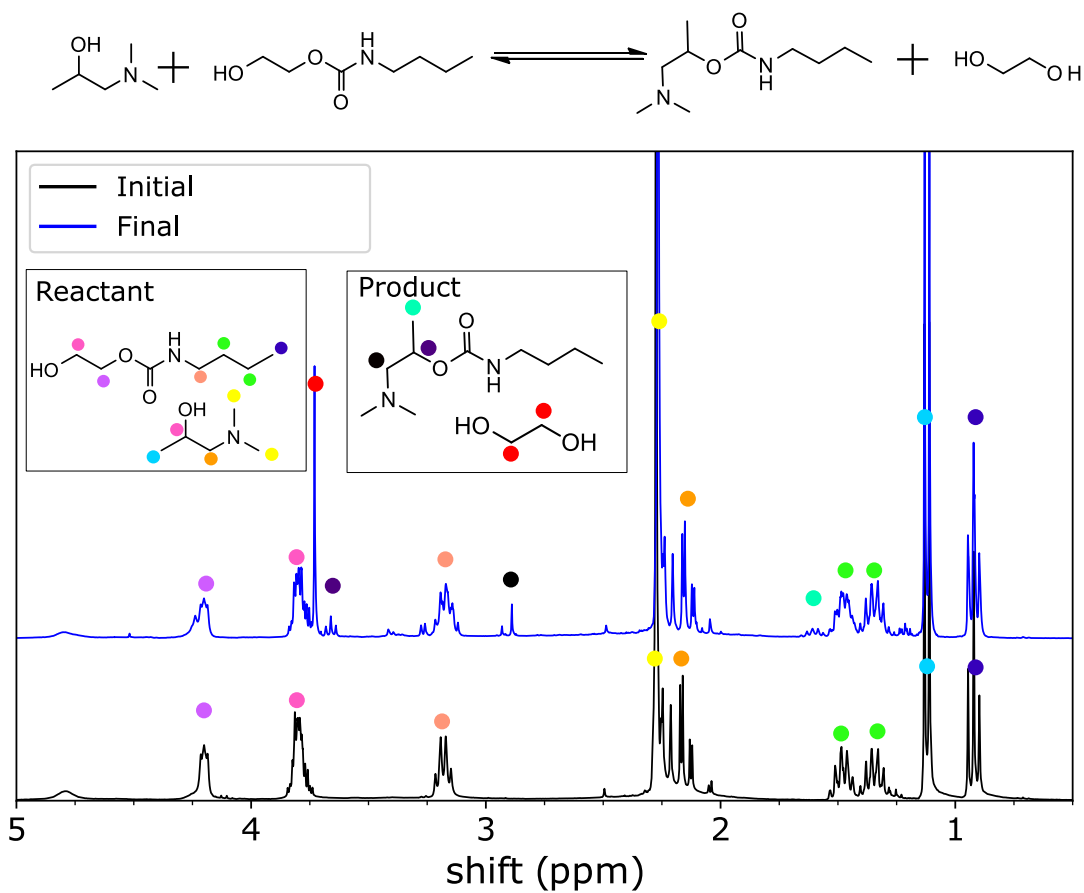
Fig. S 4: ^{1}H-NMR in CDCl$_3$ of the 2-hydroxyethyl n-butylcarbamate model compound with 1-dimethylamino-2-propanol mimicking the epoxy compound before and after 24 h at 120 °C

II.1.3 Kinetics Exchange reaction self-catalyzed
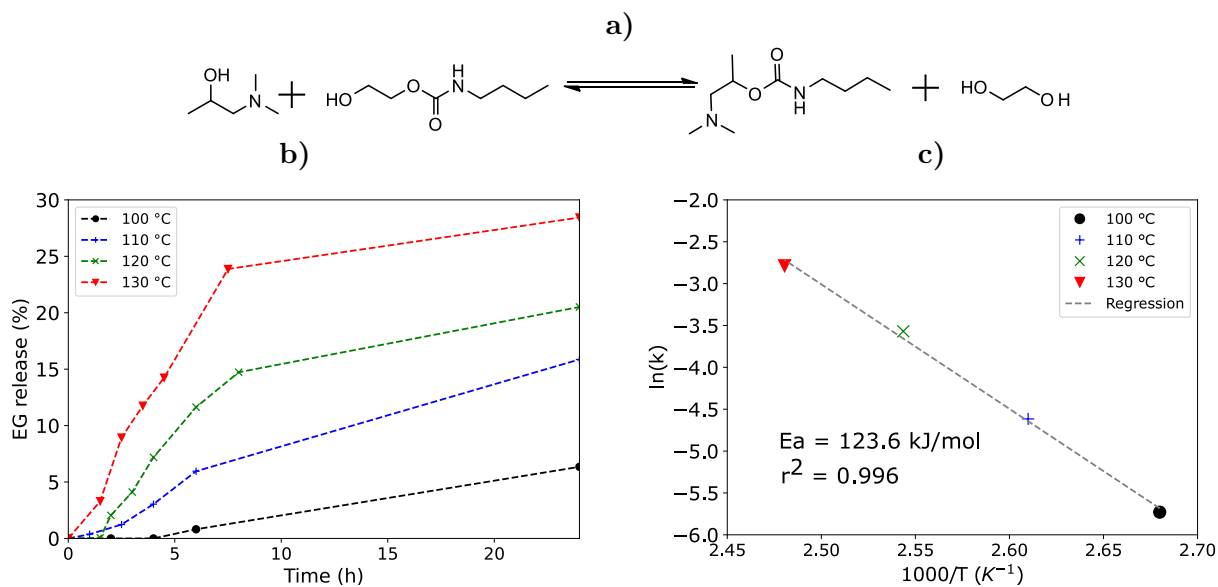
Fig. S 5: Kinetic of Ethylene Glycol (EG) release at different temperatures obtained by ^{1}H-NMR in CDCl$_3$ of the 2-hydroxyethyl n-butylcarbamate model compound with 1-dimethylamino-2-propanol mimicking the epoxy compound. a) Model reaction, b)kinetic plot, and c) Arrhenius graph with linear regression.
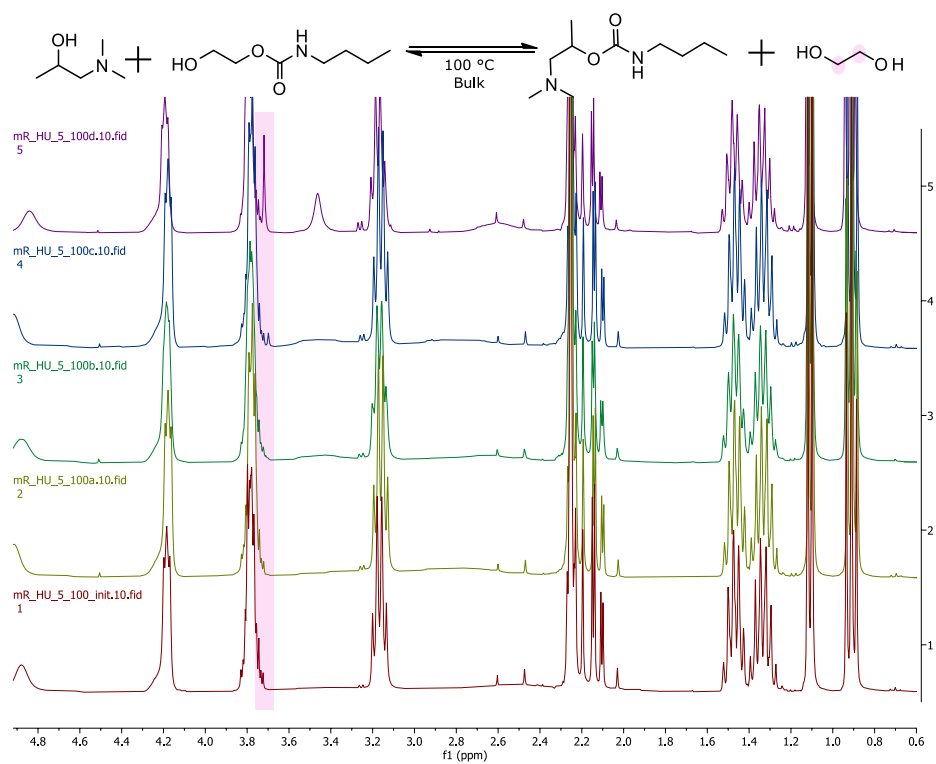
Fig. S 6: ^{1}H-NMR kinetic model reaction in CDCl$_3$. Ethylene Glycol (EG) release at 100°C temperatures obtained by ^{1}H-NMR in CDCl$_3$ of the 2-hydroxyethyl n-butylcarbamate model compound with 1-dimethylamino-2-propanol mimicking the epoxy compound.
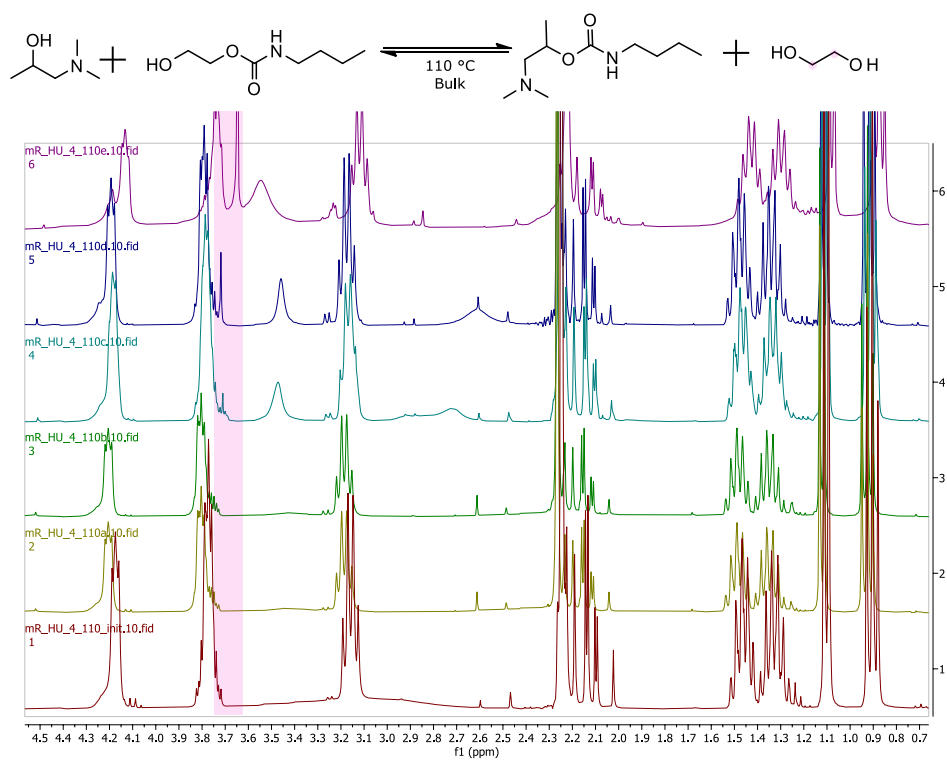
Fig. S 7: ^{1}H-NMR kinetic model reaction in CDCl$_3$. Ethylene Glycol (EG) release at 110°C temperatures obtained by ^{1}H-NMR in CDCl$_3$ of the 2-hydroxyethyl n-butylcarbamate model compound with 1-dimethylamino-2-propanol mimicking the epoxy compound.
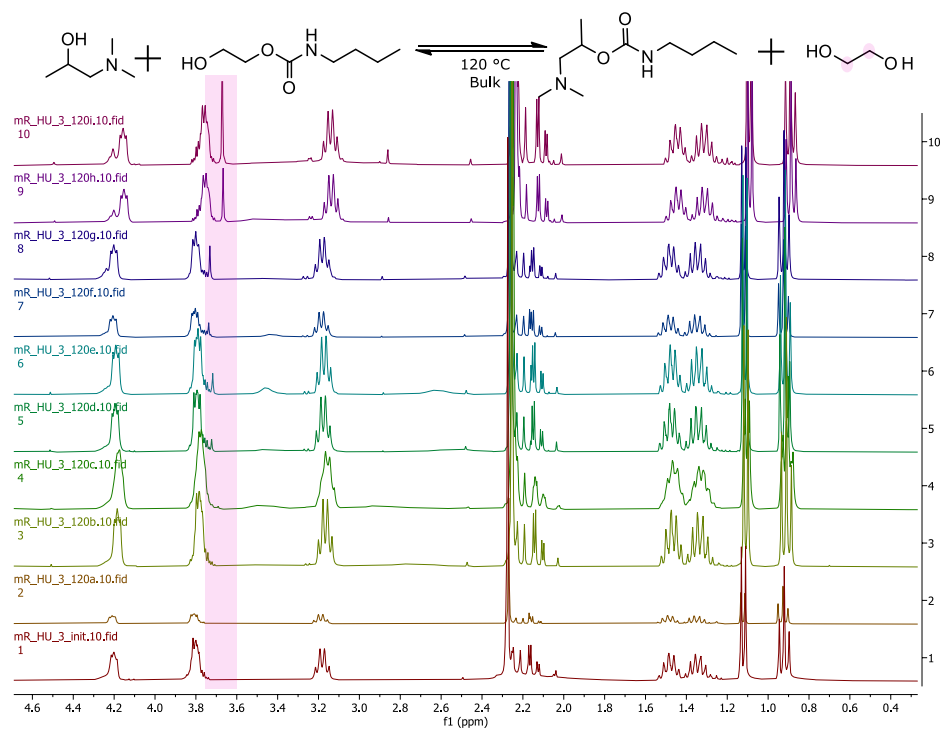
Fig. S 8: ^{1}H-NMR kinetic model reaction in CDCl$_3$. Ethylene Glycol (EG) release at 120°C temperatures obtained by ^{1}H-NMR in CDCl$_3$ of the 2-hydroxyethyl n-butylcarbamate model compound with 1-dimethylamino-2-propanol mimicking the epoxy compound.
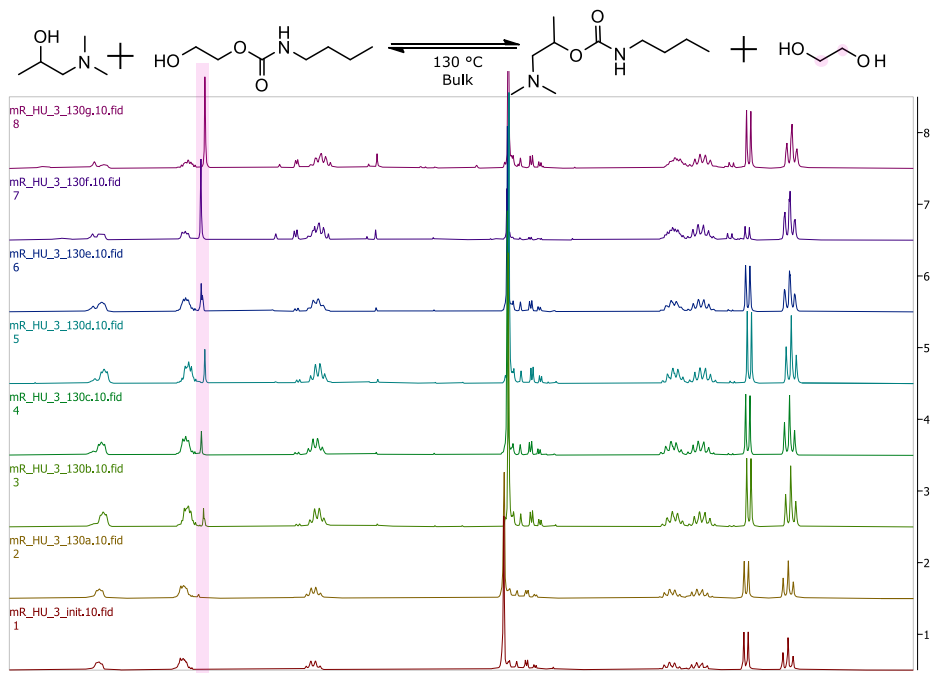
Fig. S 9: ^{1}H-NMR kinetic model reaction in CDCl$_3$. Ethylene Glycol (EG) release at 130°C temperatures obtained by ^{1}H-NMR in CDCl$_3$ of the 2-hydroxyethyl n-butylcarbamate model compound with 1-dimethylamino-2-propanol mimicking the epoxy compound.

II.1.4 Mass Spectra
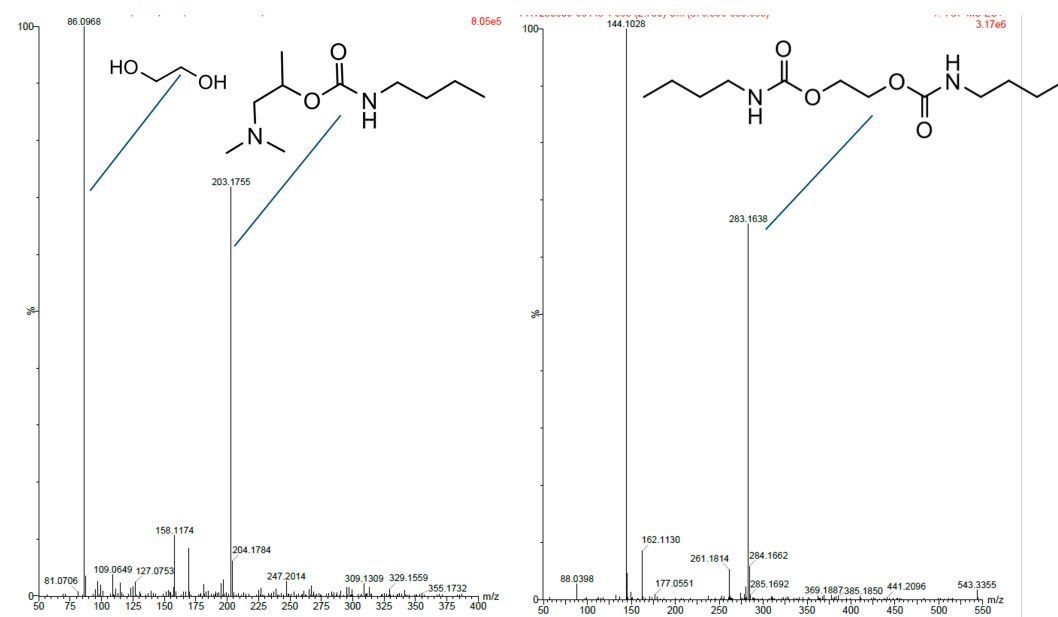
Fig. S 10: GC-MS of the model exchange reaction between 2-hydroxyethyl n-butylcarbamate model compound with 1-dimethylamino-2-propanol mimicking the epoxy compound.

II.2 Neat hybrid network properties

II.2.1 Polymerization reaction scheme
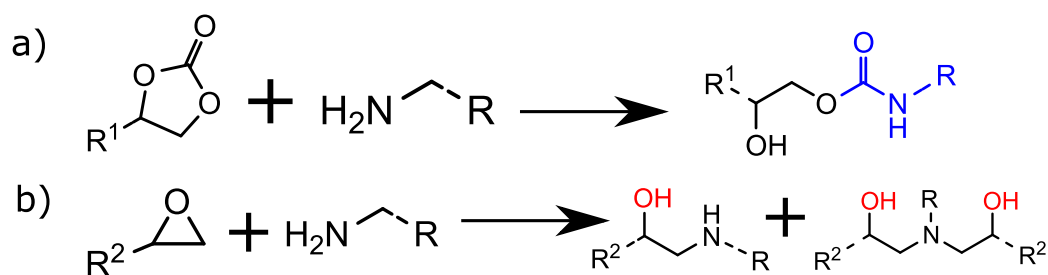
Fig. S 11: Aminolysis reaction scheme. a) Aminolysis of cyclic carbonates to hydroxyurethane moiety, and b) aminolysis of oxirane to secondary and tertiary amino-alcohol.

II.2.2   Hybrid Network Internal Structure
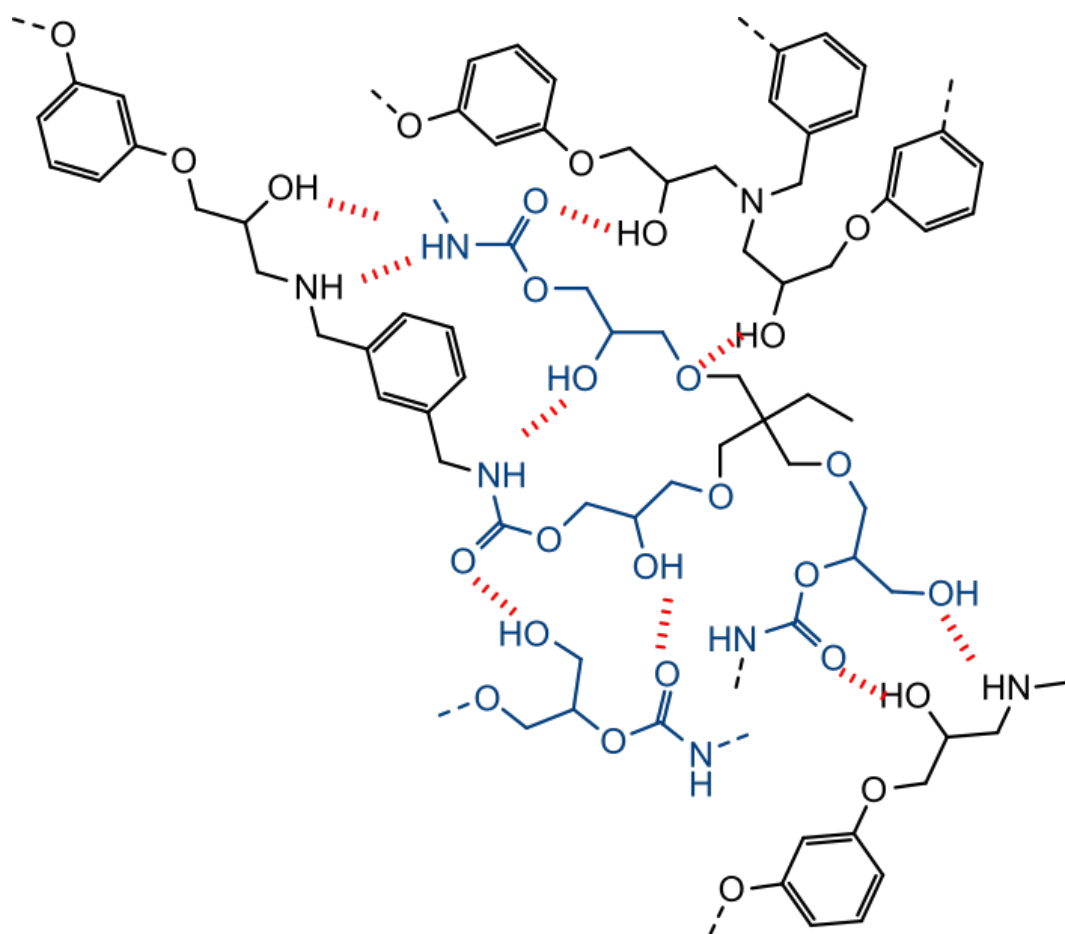
Fig. S 12: Dynamic hybrid EP internal structure. The blue backbones corresponds to PHU segments, black to epoxy-derived moieties and the red dotted lines correspond to H-bond potential sites.

II.2.3 Tensile curves and complementary results on the main formulation
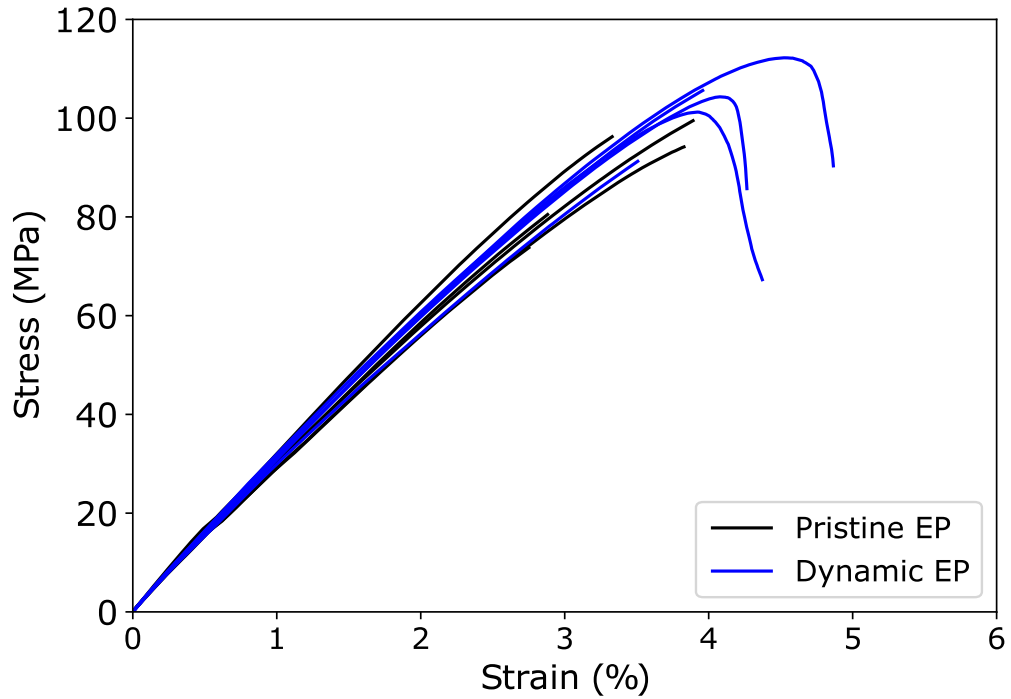
Fig. S 13: Exhaustive strain-stress curves obtained for the pristine and hybrid dynamic epoxides in tensile mode.

	ρ	SI (THF)	GC	DMA T_α	$E'_{25°C}$	$E'_{rubbery}$	ν'_e	Tensile E	σ	ϵ
	g/cm^3	%	%	°C	MPa	MPa	mol/m^3	GPa	MPa	%
Pristine EP	1.24 ± 0.01	28.1 ± 2.1	99.8 ± 0.3	97.3	2560	15.60	1519	2938 ± 98	88.8 ± 9.9	3.34 ± 0.47
Dynamic Hybrid EP	1.26 ± 0.01	5.7 ± 0.4	99.7 ± 0.3	93.6	4491	6.76	664	3061 ± 71	102.9 ± 6.8	3.99 ± 0.32

Tab. S 1: Neat Epoxy and Hybrid dynamic network properties (mean ± standard deviation)

II.2.4 Additional formulations and stress relaxation informations
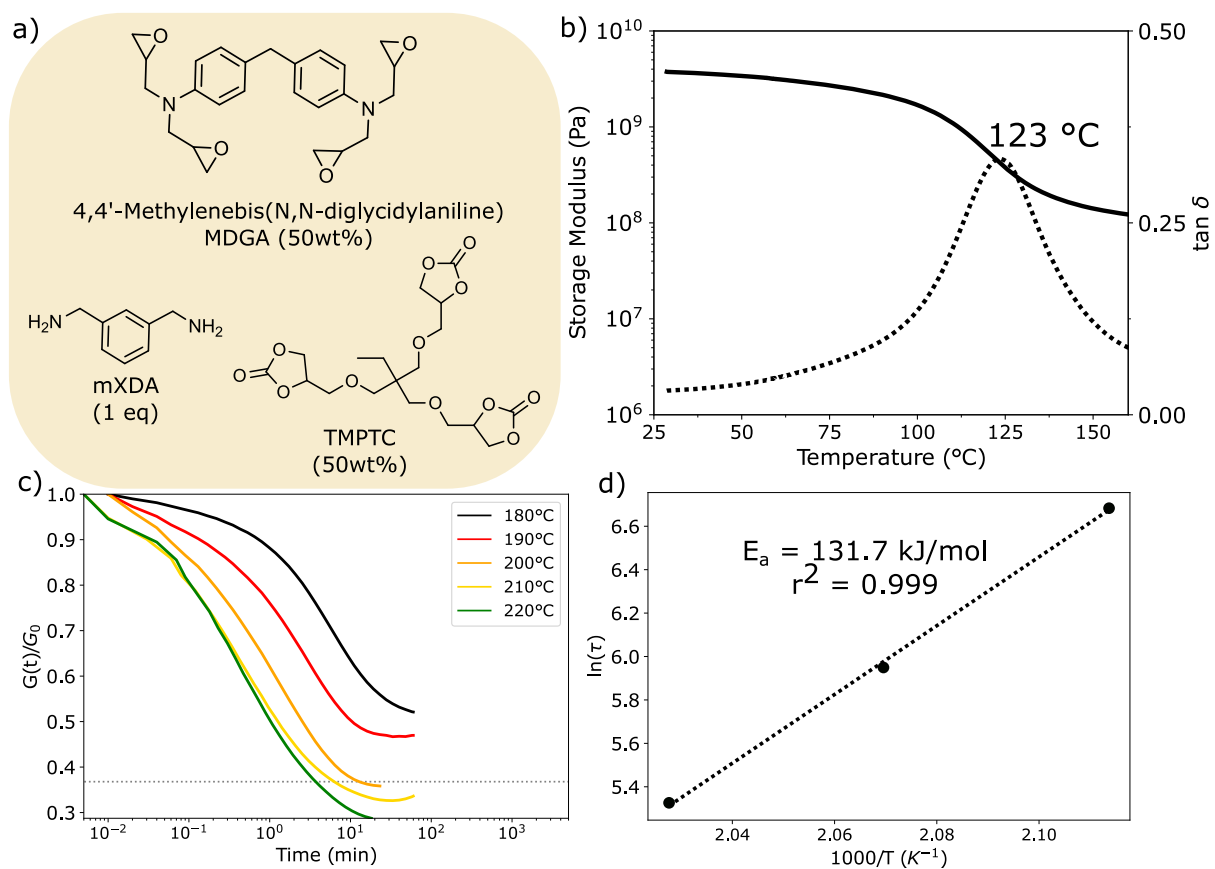
Fig. S 14: Additional formulation with high glass transition, referred to as MTX. a) Monomer structure and formulation, b) DMA of the hybrid dynamic network, c) stress relaxation of the samples, and d) Arrhenius plot.
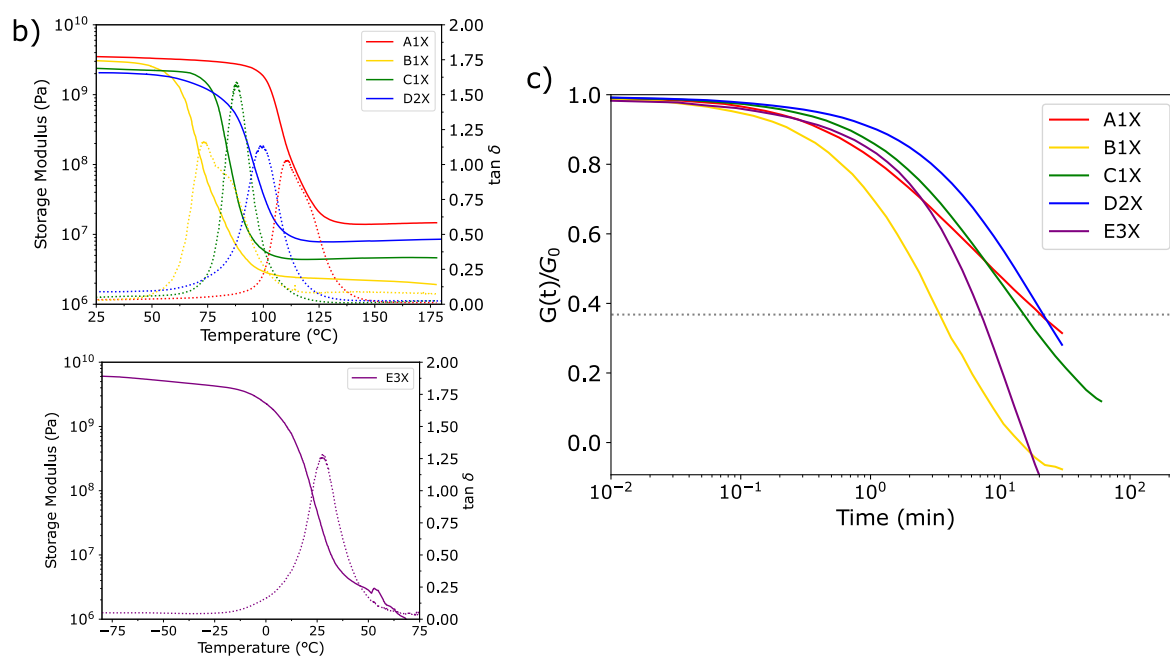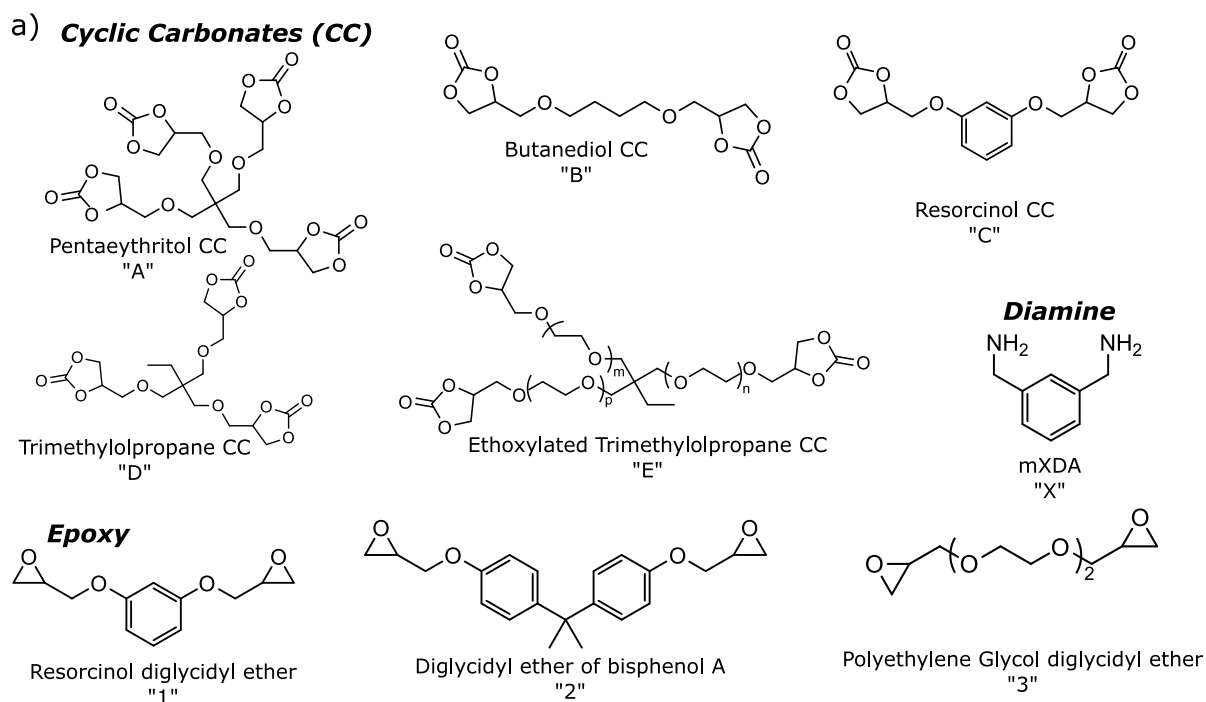
Fig. S 15: Additional formulation. a) Monomer structure, b) DMA of the hybrid dynamic networks, and c) stress relaxation of the samples at 180 $°C$ except A1X at 200 $°C$.

| | DMA | | | | Stress Relaxation |
| | T_α | $E'_{25°C}$ | $E'_{rubbery}$ | ν'_e | τ (T°C) |
	°C	MPa	MPa	mol.m^{-3}	min
MTX	123	3752	106	9526	13 min (200°C)
					6 min (210°C)
					3.4 min (220°C)
A1X	110	3506	14	1321	22 min (200°C)
B1X	73	2915	2.40	237	3.5 min (180°C)
C1X	88	2379	4.50	441	15 min (180°C)
D2X	99	2058	8.03	762	22 min (180°C)
E3X	27	48	2.72	311	7 min (180°C)

Tab. S 2: Other hybrid formulation thermomechanical and stress relaxation properties

%Carbonate	T_α (°C)	ν'_e (mol/m^3)	$\tau_{180°C}$ min
0	97	1519	-
10	98	1577	nc (>60)
25	87	663	18
50	94	664	7
75	85	613	15
90	90	1095	nc (>60)
100	78	657	237

Tab. S 3: Thermomechanical properties and stress relaxation of the dynamic epoxy (RDGE-TMPTC-mXDA) with different carbonate content.
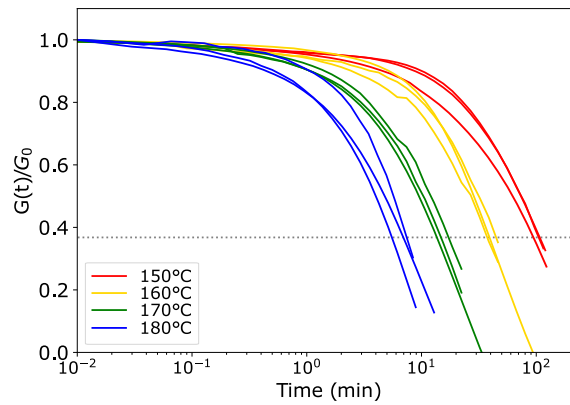
Fig. S 16: Stress relaxation experiments of the hybrid EP (50%RDGE-50%TMPTC) at 150 °C, 160 °C, 170 °C, and 180 °C

II.3 Reprocessed sample and dynamic behavior - additional results
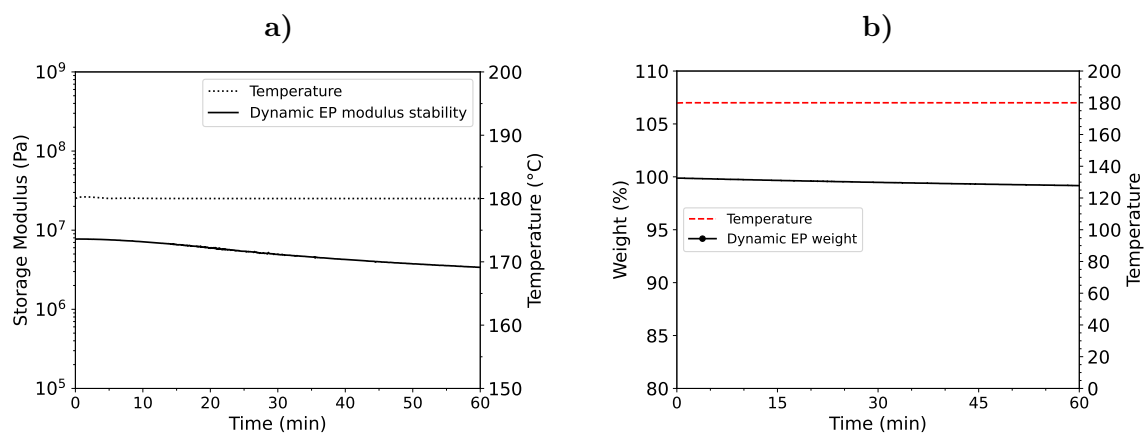
Fig. S 17: Thermal stability assesment of the dynamic EP. a) Storage modulus evolution at 180 °C, and b) Thermal weight stability at 180 °C.

Fig. S 18: Swelling in THF for 6 weeks of the reprocessed hybrid dynamic epoxy.

TM3030Plus N MU x60 1 mm
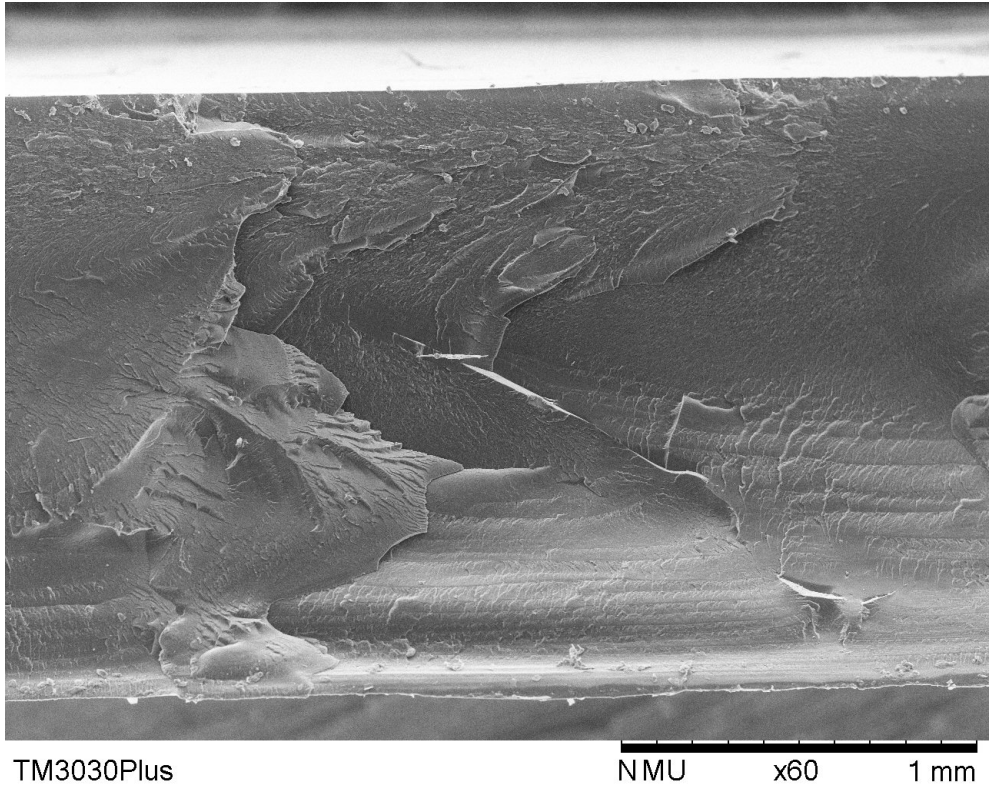
Fig. S 19: SEM images of the reprocessed hybrid dynamic epoxy after cryobreaking.
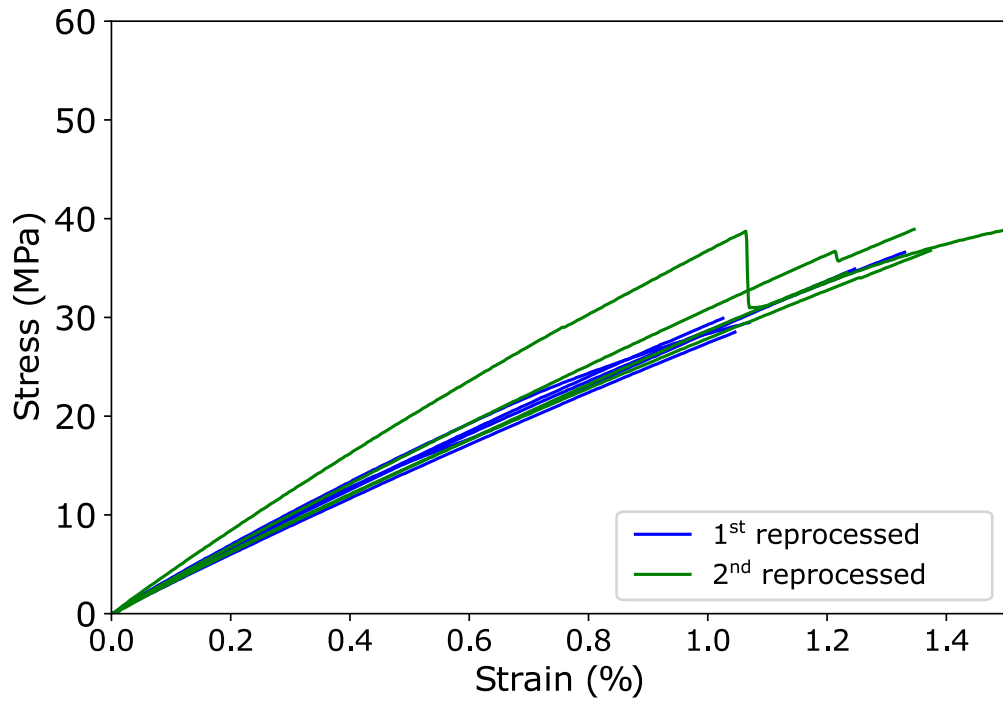
Fig. S 20: Tensile testing of the reprocessed pure hybrid dynamic polymer.

	DMA				Tensile		
	T_α ($^\circ C$)	$E'_{25^\circ C}$ (MPa)	$E'_{rubbery}$ (MPa)	ν'_e (mol/m^3)	E (GPa)	σ (MPa)	ϵ (%)
1st reprocess	93.2	3262	4.12	396	2.8 ± 0.1	31.9 ± 3.2	1.1 ± 0.1
2nd reprocess	96.8	3765	4.18	399	3.1 ± 0.3	37.5 ± 2.0	1.4 ± 0.1

Tab. S 4: Reprocessing of the hybrid dynamic network

II.4 End-of-life of composites

II.4.1 Thermomechanical recycling
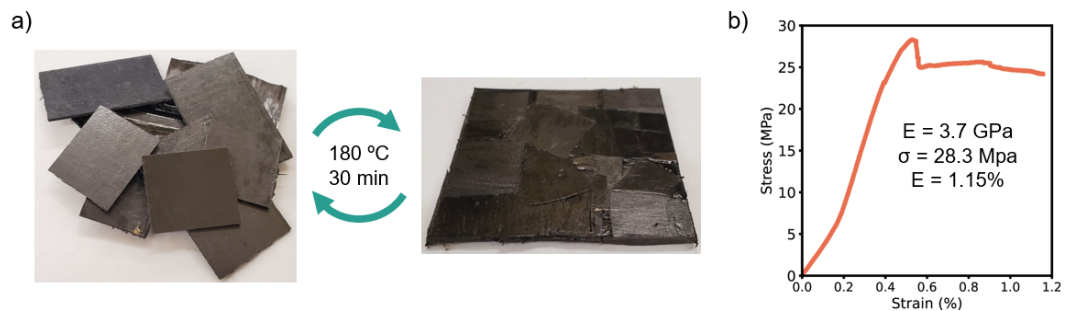
Fig. S 21: Thermomechanical recycling of the carbon fiber reinforced composites with the hybrid dynamic matrix.

II.4.2 Recovered Carbon Fibers - Additional results
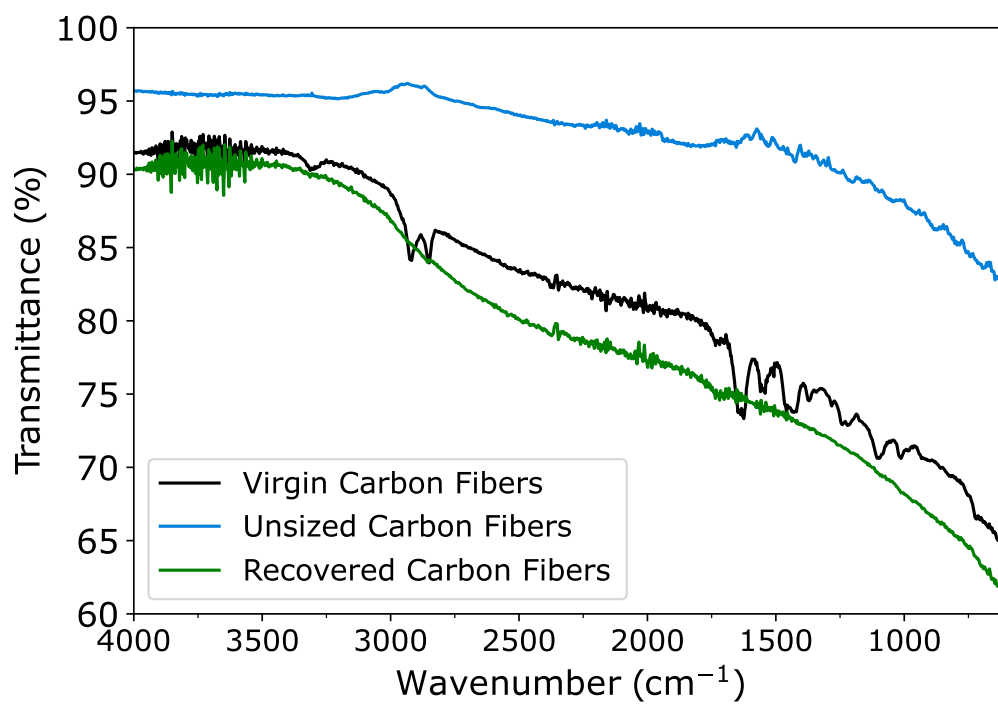
Fig. S 22: FTIR spectra of the virgin and recovered carbon fibers
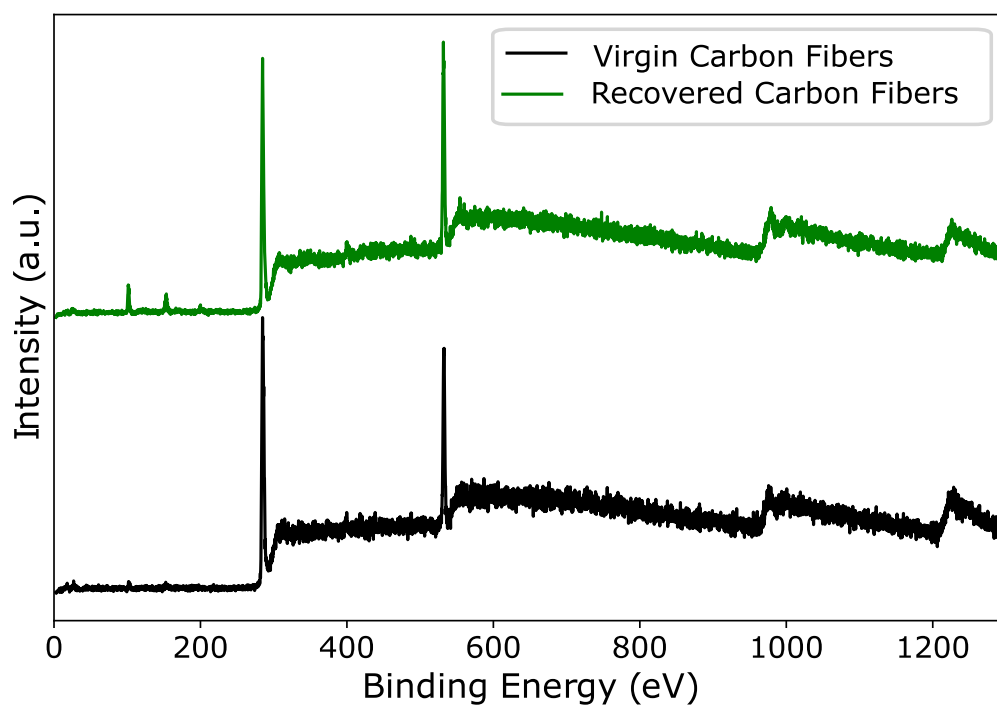
Fig. S 23: XPS, survey composition of the virgin and recovered carbon fibers

Element	Name	Position	FWHM	Library RSF	Raw Area	Area/(RSF*T*MFP)	%At Conc	% Atomic rel
C	C-C, C-H	284.60	1.46	0.314	3895.76	540.11	48.62	77.65
	C-N, C-O	286.26	1.67	0.314	2327.03	322.52	29.03	
O	O1s	531.03	1.77	0.733	314.76	17.86	1.61	19.89
	O1s	532.580	1.77	0.73	3579.59	203.07	18.28	
N*	N1s	399.50	2.01	0.499	241.82	20.65	1.86	1.86
Si*	Si2p	102.06	1.71	0.429	64.01	6.72	0.60	0.60

* Espectro cercano al ruido, estimación

Tab. S 5: XPS results for virgin carbon fibers

Element	Name	Position	FWHM	Library RSF	Raw Area	Area/(RSF*T*MFP)	%At Conc	% Atomic rel
C	C-C, C-H	284.63	1.30	0.314	5835.30	809.04	45.46	68.87
	C-N, C-O	286.12	1.50	0.314	2466.41	341.86	19.21	
	N-C=O, O-C=O	288.65	1.88	0.314	539.33	74.72	4.20	
O	O1s	531.98	1.73	0.733	5710.72	324.02	18.21	23.76
	O1s	533.20	1.73	0.733	1741.43	98.79	5.55	
N	N1s	399.79	1.88	0.499	687.60	58.73	3.30	3.30
Si	Si2p	102.05	1.54	0.429	644.97	67.71	3.80	3.80
Cl*	Cl (2p 3/2)	200.28	1.340	1.08	80.94	3.31	0.19	0.280
	Cl (2p 1/2)	201.880	1.340	1.082	40.47	1.65	0.09	

* Espectro cercano al ruido, estimación

Tab. S 6: XPS results for recovered carbon fibers
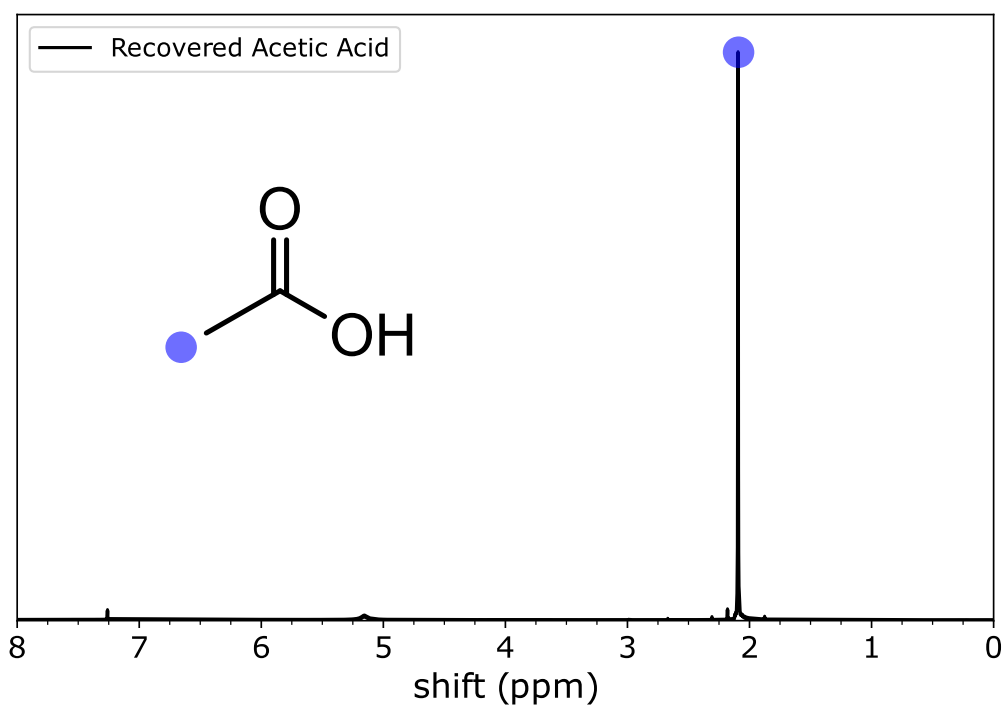
Fig. S 24: H-NMR in CDCl$_3$ of the recovered Acetic Acid after depolymerization, filtration, and evaporation. Acetic acid (CDCl$_3$,ppm) : 2.09 (s,CH$_3$)

II.5 Benchmark & Comparison with other CAN and CFRP
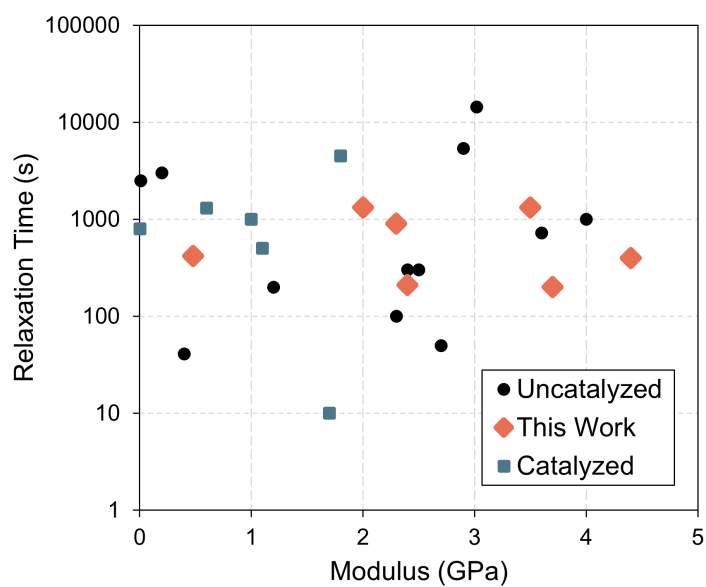
Fig. S 25: Comparative plot of the stress relaxation versus modulus of differents CANs found in literature vs this work.

Ref	Chemistry	Catalyst	$E_{25°C}$ GPa	T_g °C	τ^* s	Rel.Temp. °C
THIS WORK	Epoxy/PHU	-	3.7	123	200	220
		-	3.5	110	1320	200
		-	4.4	94	400	180
		-	2.4	73	210	180
		-	0.5	27	420	180
		-	2.3	88	900	180
		-	2	99	1320	180
[4]	Epoxy/Amine- Disulfide	-	2.7	232	50	245
[5]	Benzoxazine/transesterification	-	-	113	2012	150
[1]	Polyhydroxyurethane (PHU)	-	3.0	60	14400	180
	PHU	-	3.6	80	720	180
	PHU	-	2.9	54	5400	180
[6]	Boronic Ester crosslink of copolymer	-	0.2	180	3000	262
[7]	Benzoxazine/transesterification	-	2.5	132	301	160
	Benzoxazine/transesterification	-	0.4	65	41	160
[8]	Vinylogous urethane	-	2.4	87	300	140
[9]	Boronic Ester	-	0.01	0	2500	160
[10]	PHU	-	1.2	54	200	180
[11]	Epoxy/amine - disulfide	-	nc	176	500	185
[12]	Epoxy/amine disulfide	-	nc	147	1000	160
[13]	Benzoxazine/transesterification	-	4	143	1000	180
[14]	Epoxy / Ester	-	2.3	86	100	180
[15]	Epoxy/Amine -Siloxane	TBD (10mol%)	nc	57	100	180
[16]	N,S-Acetal	MSA (5mol%)	1.7	44	10	75
[17]	Oxime	MSA (5mol%)	nc	-29	200	150
[18]	Epoxy Acid	TBD (5mol%)	1	18	1000	180
[19]	PU	DBTDL (1mol%)	nc	50	30	140
[20]	PHU	DBTDL (2 mol%)	0.01	10	800	160
[21]	Epoxy/Ester	Zn(ac)2 (5mol%)	1.8	57	4500	190
[22]	Unsaturated Polyester	Titanium butoxide (2.0wt%)	1.1	70	500	180
[23]	Epoxy/Ester	Zn2+ Ionomer (5mol%)	0.6	43	1300	170

Tab. S 7: Comparison of different dynamic chemistries performance
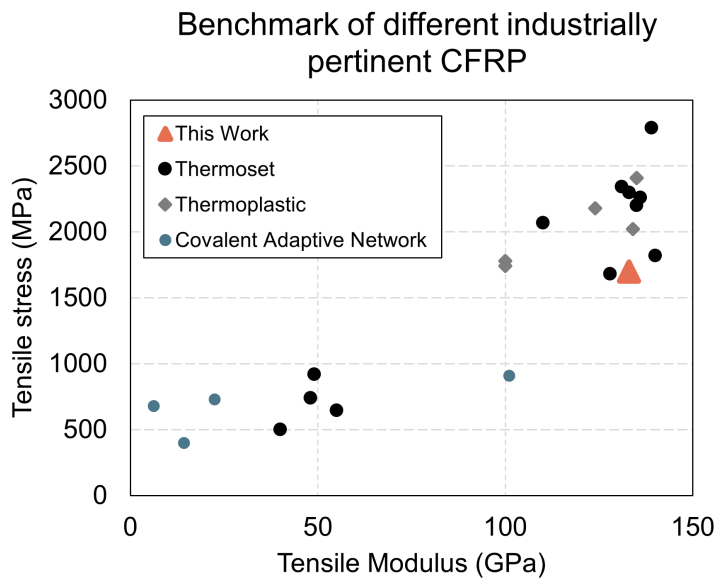
Fig. S 26: Comparative plot of CFRP modulus versus ultimate stress found in literature or commercially available, using thermoset, thermoplastic and CAN matrices.

	Name/ref	Supplier	Fibre	Matrix	T_g °C	E GPa	σ MPa	Recyclable	Catalyst
CAN	This work		Carbon	EP/PHU	27-130	133	1700	Yes	no
	[24]		Woven Carbon	Polyimine (PI)	60-145	14.2	400	Yes	no
	[25]		Woven Carbon	EP/PI	135-147	6.2	681	Yes	DMAP
	[26]		UD Carbon	UPR	150	101	910	Yes	Ti(IV)
	[6]		Woven Carbon	Modified SBpin	180	22.370	731	Yes	no
Thermoset	XC130 150 g UD Prepreg	Easy Composite	UD Carbon	Epoxy	140	55	645	no	-
	Carbon Fibre Strip	Easy Composite	UD Carbon	Vinyl Ester	80	40	500	no	-
	HexPly®8552 - AS4 Fibers	Hexcel	UD Carbon	Epoxy	200	135	2200	no	-
	HexPly®8552 - AS7 Fibers	Hexcel	UD Carbon	Epoxy	200	133	2300	no	-
	Conventional Pre-preg	Toray	UD Carbon	Epoxy	nc	49	920	no	-
	ET40	Toray	UD Carbon	Epoxy	nc	48	740	no	-
	2300 Prepreg system	Toray	UD Carbon	Epoxy	148	139	2790	no	-
	2510/P707AG-15	Toray	UD Carbon	Epoxy	146	128	1682	no	-
	T300/EP2500 Toray	Toray	UD Carbon	Epoxy	nc	140	1820	no	-
	Prepreg 316	Mitsubishi	UD Carbon	Epoxy	115	136	2260	no	-
	HMT317	Mitsubishi	UD Carbon	Epoxy	125	110	2070	no	-
	Prepreg 350	Mitsubishi	UD Carbon	Epoxy	192	131	2344	no	-
Thermoplastic	VESTAPE-PA12	Evonik	UD Carbon	PA12	40	100	1740	Yes	-
	VESTAPE-PEEK	Evonik	UD Carbon	PEEK	151	100	1780	Yes	-
	Toray Cetex®TC1320	Toray	UD Carbon	PEKK	160	135	2410	Yes	-
	Toray Cetex®TC915	Toray	UD Carbon	PA6	75	124	2179	Yes	-
	Toray Cetex®TC1200 P	Toray	UD Carbon	PEEK	143	135	2410	Yes	-
	Toray Cetex®TC1100	Toray	UD Carbon	PPS	90	134	2020	Yes	-

Tab. S 8: Comparison of different vitrimer & commercially available carbon fiber composites

References

[1] Guillem Seychal, Connie Ocando, Leila Bonnaud, Julien De Winter, Bruno Grignard, Christophe Detrembleur, Haritz Sardon, Nora Aramburu, and Jean-Marie Raquez. Emerging Polyhydroxyurethanes as Sustainable Thermosets: A Structure–Property Relationship. *ACS Applied Polymer Materials*, 5(7):5567–5581, June 2023.

[2] Stefan Grimme, Stephan Ehrlich, and Lars Goerigk. Effect of the damping function in dispersion corrected density functional theory. *Journal of Computational Chemistry*, 32(7):1456–1465, May 2011.

[3] Brent H. Besler, Kenneth M. Merz Jr., and Peter A. Kollman. Atomic charges derived from semiempirical methods. *Journal of Computational Chemistry*, 11(4):431–439, 1990. _eprint: https://onlinelibrary.wiley.com/doi/pdf/10.1002/jcc.540110404.

[4] Vincent Schenk, Raffaele D'Elia, Philippe Olivier, Karine Labastie, Mathias Destarac, and Marc Guerre. Exploring the Limits of High- T_g Epoxy Vitrimers Produced through Resin-Transfer Molding. *ACS Applied Materials & Interfaces*, 15(39):46357–46367, October 2023.

[5] Henri Perrin, Régis Vaudemont, Doriane Del Frari, Pierre Verge, Laura Puchot, and Masoud Bodaghi. On the cyclic delamination-healing capacity of vitrimer-based composite laminates. *Composites Part A: Applied Science and Manufacturing*, 177:107899, February 2024.

[6] Md Anisur Rahman, Menisha S. Karunarathna, Christopher C. Bowland, Guang Yang, Catalin Gainaru, Bingrui Li, Sungjin Kim, Vivek Chawla, Natasha Ghezawi, Harry M. Meyer, Amit K. Naskar, Dayakar Penumadu, Alexei P. Sokolov, and Tomonori Saito. Tough and recyclable carbon-fiber composites with exceptional interfacial adhesion via a tailored vitrimer-fiber interface. *Cell Reports Physical Science*, 4(12):101695, December 2023.

[7] Guillem Seychal, Louis Van Renterghem, Connie Ocando, Leila Bonnaud, and Jean-Marie Raquez. Towards sustainable reprocessable structural composites: Benzoxazines as biobased matrices for natural fibers. *Composites Part B: Engineering*, 272:111201, March 2024.

[8] Wim Denissen, Guadalupe Rivero, Renaud Nicolaÿ, Ludwik Leibler, Johan M. Winne, and Filip E. Du Prez. Vinylogous Urethane Vitrimers. *Advanced Functional Materials*, 25(16):2451–2457, April 2015.

[9] Yingjun Liu, Zhenghai Tang, Yi Chen, Chengfeng Zhang, and Baochun Guo. Engineering of beta-Hydroxyl Esters into Elastomer–Nanoparticle Interface toward Malleable, Robust, and Reprocessable Vitrimer Composites. *ACS Applied Materials & Interfaces*, 10(3):2992–3001, January 2018.

[10] David J. Fortman, Jacob P. Brutman, Christopher J. Cramer, Marc A. Hillmyer, and William R. Dichtel. Mechanically Activated, Catalyst-Free Polyhydroxyurethane Vitrimers. *Journal of the American Chemical Society*, 137(44):14019–14022, November 2015.

[11] Alaitz Ruiz De Luzuriaga, Nerea Markaide, Asier M. Salaberria, Itxaso Azcune, Alaitz Rekondo, and Hans Jürgen Grande. Aero Grade Epoxy Vitrimer towards Commercialization. *Polymers*, 14(15):3180, August 2022.

[12] Hongwei Si, Lin Zhou, Yeping Wu, Lixian Song, Ming Kang, Xiuli Zhao, and Mao Chen. Rapidly reprocessable, degradable epoxy vitrimer and recyclable carbon fiber reinforced thermoset composites relied on high contents of exchangeable aromatic disulfide crosslinks. *Composites Part B: Engineering*, 199:108278, October 2020.

[13] Antoine Adjaoud, Laura Puchot, and Pierre Verge. High-Tg and Degradable Isosorbide-Based Polybenzoxazine Vitrimer. *ACS Sustainable Chemistry & Engineering*, 10(1):594–602, January 2022.

[14] Yazhou Xu, Songlin Dai, Liangwu Bi, Jianxin Jiang, Haibo Zhang, and Yuxiang Chen. Catalyst-free self-healing bio-based vitrimer for a recyclable, reprocessable, and self-adhered carbon fiber reinforced composite. *Chemical Engineering Journal*, 429:132518, February 2022.

[15] Tapas Debsharma, Virginia Amfilochiou, Aleksandra Alicja Wróblewska, Ives De Baere, Wim Van Paepegem, and Filip E. Du Prez. Fast Dynamic Siloxane Exchange Mechanism for Reshapable Vitrimer Composites. *Journal of the American Chemical Society*, 144(27):12280–12289, July 2022.

[16] Thomas Habets, Guillem Seychal, Marco Caliari, Jean-Marie Raquez, Haritz Sardon, Bruno Grignard, and Christophe Detrembleur. Covalent adaptable networks through dynamic N,S-acetal chemistry: toward recyclable CO2-based thermosets. *Journal of the American Chemical Society*, 145(46):25450–25462, September 2023.

[17] Luca Pettazzoni, Marta Ximenis, Francesca Leonelli, Giulia Vozzolo, Enrico Bodo, Fermin Elizalde, and Haritz Sardon. Oxime metathesis: tuneable and versatile chemistry for dynamic networks. *Chemical Science*, 15(7):2359–2364, 2024.

[18] Jianqiao Wu, Xia Yu, Hao Zhang, Junbo Guo, Jun Hu, and Min-Hui Li. Fully Biobased Vitrimers from Glycyrrhizic Acid and Soybean Oil for Self-Healing, Shape Memory, Weldable, and Recyclable Materials. *ACS Sustainable Chemistry & Engineering*, 8(16):6479–6487, April 2020. Publisher: American Chemical Society.

[19] David J. Fortman, Daylan T. Sheppard, and William R. Dichtel. Reprocessing Cross-Linked Polyurethanes by Catalyzing Carbamate Exchange. *Macromolecules*, 52(16):6330–6335, August 2019.

[20] Camille Bakkali-Hassani, Dimitri Berne, Pauline Bron, Lourdes Irusta, Haritz Sardon, Vincent Ladmiral, and Sylvain Caillol. Polyhydroxyurethane covalent adaptable networks: looking for suitable catalysts. *Polymer Chemistry*, 14(31):3610–3620, 2023.

[21] Damien Montarnal, Mathieu Capelot, François Tournilhac, and Ludwik Leibler. Silica-Like Malleable Materials from Permanent Organic Networks. *Science*, 334(6058):965–968, November 2011.

[22] Giuliana Rizzo, Lorena Saitta, Sandro Dattilo, Claudio Tosto, Eugenio Pergolizzi, Alojz Ivankovic, and Gianluca Cicala. Thermomechanical Characterization of an Unsaturated Polyester Vitrimer Synthesized Using a Titanium Transesterification Catalyst. *ACS Applied Polymer Materials*, 5(10):8326–8338, October 2023. Publisher: American Chemical Society.

[23] Xiling Niu, Fenfen Wang, Xiaohui Li, Rongchun Zhang, Qiang Wu, and Pingchuan Sun. Using Zn2+ Ionomer To Catalyze Transesterification Reaction in Epoxy Vitrimer. *Industrial & Engineering Chemistry Research*, 58(14):5698–5706, April 2019. Publisher: American Chemical Society.

[24] Philip Taynton, Huagang Ni, Chengpu Zhu, Kai Yu, Samuel Loob, Yinghua Jin, H. Jerry Qi, and Wei Zhang. Repairable Woven Carbon Fiber Composites with Full Recyclability Enabled by Malleable Polyimine Networks. *Advanced Materials*, 28(15):2904–2909, April 2016.

[25] Pei-Xiu Tian, Yi-Dong Li, Zhi Hu, and Jian-Bing Zeng. Flame-retardant epoxy vitrimers with high strength and high-Tg for recyclable carbon fiber-reinforced composites. *Composites Communications*, 47:101870, April 2024.

[26] Giuliana Rizzo, Vishnu Prasad, Miray Yasar, Gianluca Cicala, Alojz Ivankovic, Neal Murphy, and Alberta Latteri. Investigation of mechanical properties and self-healing efficiency of carbon fibers composites infused with unsaturated polyester vitrimer. *Polymer Composites*, 45(11):10404–10417, 2024. _eprint: https://onlinelibrary.wiley.com/doi/pdf/10.1002/pc.28483.